Send Orders for Reprints to reprints@benthamscience.ae

Current Pharmaceutical Biotechnology, 2018, *19*, 000-000

RESEARCH ARTICLE

The Drug Combination of SB202190 and SP600125 Significantly Inhibit the Growth and Metastasis of Olaparib-resistant Ovarian Cancer Cell

Xinyan Chen[1,2], Yumei Chen[2], Xueyan Lin[1], Shan Su[3], Xiaoman Hou[1], Qian Zhang[1] and Yongjie Tian[1*]

[1]*Department of Obstetrics and Gynecology, Shandong Provincial Hospital Affiliated to Shandong University, No. 324 Jingwu Road, Jinan 250021, China;* [2]*Department of Gynecology and Obstetrics, Wenzhou People's Hospital, No. 57 Canghou Street, Wenzhou 325000, China;* [3]*Department of Gynecology, The Central Hospital of Zibo, No. 54 of Gongqingtuan West Road, Zibo, China*

ARTICLE HISTORY

Received: February 06, 2018
Revised: May 03, 2018
Accepted: July 02, 2018

DOI:
10.2174/1389201019666180713102656

Abstract: ***Background & Objective***: Many targeted ovarian cancer patients are resistant to olaparib treatment. Here we seek to understand the underlying molecular events and search for potential combinational therapeutics to surmount the intrinsic olaparib resistance in human ovarian cancer.

Methods: The cytotoxicity was determined by the MTT assay and cell viability was measured using Cell Counting Kit-8 (CCK-8). Protein expressions of ERK, P38, JNK, ERK5, LC3, N-CADHERIN, α-SMA were determined by western blotting. The invasion capacity was evaluated by the transwell chamber. Autophagy flux was monitored by the LC3 puncta formation. The epithelial-mesenchymal transition (EMT) markers were profiled by immunoblotting detection. The *in vivo* tumor progression was determined by xenograft mice model.

Results: The olaparib-resistant cell lines were successfully generated in both SKOV3 and A2780 cells. The proliferative index was significantly higher in resistant cells in comparison with sensitive counterparts in the presence of olaparib. Both P38 and JNK were up-regulated in olaparib-resistant cells. The combinational treatment with P38-specific inhibitor SB202190 and JUN-specific inhibitor SP600125 significantly suppressed cell growth and migration, which was further attributed to the induction of autophagy flux and inhibition of EMT processing. We further consolidated the anti-tumor activities of SB202190 and SP600125 in xenograft mice.

Conclusion: Our data suggested that aberrant over-expression of P38 and JNK is causally linked to the olaparib resistance in ovarian cancer. Combination of P38 and JUN inhibitors demonstrated significant anti-tumor activity both *in vitro* and *in vivo*. Our study highlighted the potential therapeutic value of Mitogen-Activated Protein Kinase (MAPK) inhibitors in olaparib-resistant human ovarian cancer.

Keywords: Olaparib, ovarian cancer, SB202190, SP600125, MAPK, anti-tumor.

1. INTRODUCTION

Ovarian cancer is one of the most common and malignant reproductive system tumors worldwide and is placed on third position immediately after cervical cancer and uterine cancer [1]. However, the ovarian epithelial tumor is the first cause of cancer-related death in all gynecological tumors. There were approximately 22,400 new cases diagnosed and 14,080 deaths claimed by this disease in the US in 2017 according to the Cancer Statistics 2017 [2]. The etiology study has identified risk factors closely associated with ovarian cancer including never giving birth, early ovulation, late menopause and sometimes hormone therapy, fertility medication and increasing obesity [3]. The next generation sequencing of cancer patients uncovered that about 10% of the ovarian tumor is linked to the hereditary genetic mutations in BRCA1 and BRCA2 genes [4]. The epidemiological investigation also highlighted the beneficial effect of breastfeeding against the incidence of ovarian cancer [5]. Histologically, ovarian cancer is roughly categorized into high-grade serous carcinoma, germ cell tumor and sex cord-stromal tumor. Clinically, ovarian cancer is frequently under-diagnosed at an

*Address correspondence to this author at the Department of Obstetrics and Gynecology, Shandong Provincial Hospital Affiliated to Shandong University, No. 324 Jingwu Road, Jinan 250021, China; Tel: +86-0531-87938911; E-mail: tianyongjie1516@sina.com

1389-2010/18 $58.00+.00

early stage due to atypical symptom and lack of reliable and sensitive marker. The available mainstay clinical options for ovarian cancer consist of surgery, radiotherapy, and chemotherapy [6]. Although surgery is a preferential option with curative potential, it is not applicable to the advanced cases due to the multiple metastases. For most of the aggressive and advanced tumor patients, combinational treatment with surgical removal and chemotherapy is appropriate and feasible management routine [7]. Application of radiotherapy in ovarian cancer is greatly limited in consideration of resultant infertility. The immune-checkpoint based therapeutics are under investigation and exploitation as well [8]. In general, the prognosis of ovarian cancer is relatively moderate and the overall 5-year survival rate is around 45%.

Olaparib (also known as AZD-2281, trade name Lynparza) is an FDA-approved targeted therapy for germline BRCA mutated advanced ovarian cancer that has received three or more prior lines of chemotherapy [9]. Olaparib is a poly ADP ribose polymerase (PARP) inhibitor, which specifically inhibits PARP and blocks the DNA repair processing [10]. The BRCA mutated ovarian cancer manifests increased reliance on PARP and therefore is vulnerable to PARP inhibition. The early clinical trials demonstrated significantly favorable response to olaparib in BRCA mutated ovarian cancer patients [11]. However, a proportion of targeted patients are intrinsically resistant to olaparib treatment due to unrecognized mechanisms. Moreover, like most of the targeted anti-tumor drugs, the developing resistance is apparently inevitable for olaparib. Therefore, appropriate compounds with the potential to surmount drug resistance either in combination or alone are in urgent need in the future. Here we set out to establish the olaparib-resistant ovarian cancer cells to recapitulate the whole process *in vitro* and characterize the potential candidate targets molecularly associating with resistance occurrence. Furthermore, we consolidate this notion *via* employment of specific inhibitors both *in vitro* and *in vivo*. Our data offered both experimental and preclinical significance.

2. MATERIALS AND METHODS

2.1. Cell Culture

The human ovarian cancer cell lines SKOV3 and A2780 were obtained and authenticated by the American Type Culture Collection (ATCC, VA, USA). The exponential cells were cultured in RPMI-1640 medium (Hyclone, MO, USA) containing 10% fetal bovine serum (Hyclone, MO, USA) and 1% penicillin/streptomycin (Gibco, CA, USA). Cells were maintained in the humidified CO_2 (5%) incubator at 37^oC.

2.2. Transfection

Cell transfection was performed using Lipofectamine 2000 following the provider's instruction. Briefly, the exponential cells were seeded into 6-well plate and cultured for 24 hours before transfection. 2 μg of indicated plasmids was packaged with 5 μL Lipofectamine 2000 and incubated at room temperature for 5 min. The mixture was added into each well and incubated for 24 h. The transfection efficiency was evaluated by a parallel assay with GFP.

2.3. MTT Assay

The indicated log phase cells were seeded into 96-well plate in triplicate and allowed for consecutive culture for 24 h and subjected to a different dosage of olaparib treatment. The culture medium was cautiously aspirated and 150 μl MTT solution was added into each well followed by agitation on an orbital shaker for 15 min at room temperature. The absorbance at 590 nm was measured by the microplate reader (Molecular Devices, CA, USA) and IC50 was calculated for each cell line.

2.4. Cell Proliferation

Cell proliferation was determined using the commercially available CCK-8 Kit (Dojindo, Dalian, China) in accordance with the manufacturer's instruction. Every 10^4 of indicated cells were seeded into 96-well plate in triplicate for 24 hours culture and then incubated with 10 μl of the CCK-8 solution at 37 °C for 1.5 h. The OD450 was measured by microplate reader (Molecular Devices, CA, USA) and relative cell count was calculated.

2.5. Western Blot

The indicated cells were lysed in RIPA buffer on ice for 30 min and all the debris were completely removed by high-speed centrifugation at 4^oC. The protein concentration was quantified using the BCA Protein Assay Kit (ThermoFisher, MA, USA). Protein was resolved by SDS-PAGE and then transferred onto PVDF membrane on ice. After brief blocking with skim milk (5% in TBST buffer with 0.05% Tween-20), the PVDF membrane was incubated with specific antibodies (anti-ERK, CST#9102, 1:1,000; anti-P38, CST#8690, 1:1,000; anti-JNK, CST#9252, 1:1,000; anti-ERK5, CST#3372, 1:1,000; anti-ACTIN, CST#4970, 1:1,000; anti-LC3A/B, CST#4108, 1:1,000; anti-N-CADHERIN, CST#4061, 1:1,000; anti-α-SMA, CST#14968, 1:1,000) at 4^oC overnight. The excessive antibody was completely washed off with TBST for 30 min and followed by secondary antibody (anti-mouse, CST#7076, 1:5,000; anti-rabbit, CST#7074, 1:5,000;) incubation. The protein was visualized by the application of the enhanced chemiluminescence (ECL, Millipore, CA, USA) kit. The endogenous acting was employed for loading control purpose.

2.6. Transwell Assay

The metastatic capacity of ovarian cancer cells was evaluated *in vitro* using the transwell chamber (BD Biosciences, CA, USA). The cells were first starved in serum-free medium for 24 hours, then digested into single-cell solution at a concentration of 1×10^5/100 μL in serum-free medium and laid on the top of polycarbonate Transwell filter, which was pre-coated with Matrigel (BD Biosciences, CA, USA). The lower compartment was filled with 750 μL of complete culture medium containing 10% fetal bovine serum. 24 hours later, the upper compartment was cleared up with cotton Q-tips. The invaded cells were then fixed with 4% paraformaldehyde and stained with 0.025 % crystal violet solution for 25 min. The cells were counted in three random fields under a light microscope.

2.7. Autophagy Puncta Imaging

The SKOV3 and A2780 cells were first transfected and labeled with GFP-LC3. The cells subjected to the indicated treatment were fixed with 4% paraformaldehyde and stained with DAPI for nuclear imaging. Autophagy flux was examined with a confocal microscope (Nikon i2, Japan).

2.8. Xenograft Model

The 4~6-week-old immunodeficient NPG mice were obtained from Shanghai Liangtai Company (Shanghai, China) and acclimated for one week in the pathogen-free environment. All the animal studies were performed in accordance with the protocol approved by the Animal Care and Use Committee of Shandong Provincial Hospital Affiliated to Shandong University. Briefly, the single-cell suspension (10^7 cells/mL in HEPES) was prepared by trypsin digestion and mixed well with an equal volume of Basement Membrane Extracts (R&D System, MN, USA) on ice. The mixture was subcutaneously inoculated into bilateral flanks of recipient mice immediately. The tumor growth was monitored regularly and the tumor volume was calculated using the following formula: Volume = $(\text{width})^2 \times \text{length}/2$.

2.9. Statistics

Data expressed in this study were obtained from at least three independent experiments unless indicated. Data were processed and analyzed using PRISM 7.0 software and presented as mean ± standard deviation (S.D.). The one-way analysis of variance (ANOVA) followed by *t*-test was employed for statistical comparison. The statistical significances were calculated as p values, and $P < 0.05$ was considered statistically different.

3. RESULTS

3.1. P38 and JNK are Overexpressed in Olaparib-resistant Ovarian Cancer Cells

To investigate the olaparib resistance in ovarian cancer *in vitro*, here we first established olaparib resistance cell lines in both human ovarian cancer SKOV3 and A2780 cells (denoted as SKOVE-R and A2789-R respectively). Both the cells were challenged with interval and increasing concentration of olaparib. The success to establish resistant cell lines was confirmed by measurement of IC50 of olaparib using MTT assay. As shown in Fig. (**1A**), IC50 value increased to 415 ± 12 μM in A2780-R in comparison with 16 ± 5 μM in the parental A2780-P cells, while 688 ± 22 μM vs. 25 ± 17 μM in SKOV3 cells (the detailed MTT results were supplemented in Figure S1). The cell proliferation upon olaparib treatment was determined by the CCK-8 method. Olaparib administration significantly suppressed cell growth in both SKOV3-P (25 μM) and A2780-P (15 μM) cells, while none of the significant influence was observed in the resistant cell lines (Fig. **1B**). We further characterized the alteration in the MAPK signaling pathway in the resistant cell lines in comparison with sensitive counterparts. As shown in Fig. (**1C**) and D, both P38 and JNK were significantly up-regulated in SKOV3-R and A2780-R, which indicated a potential contribution of this signaling to the drug resistance.

3.2. P38 and JNK Inhibition Significantly Decrease the Proliferation and Metastasis of Olaparib-resistant Ovarian Cancer Cells

Our primary results demonstrated the aberrant overexpression of MAPKs in olaparib-resistant cells, which prompted us to investigate the potential anti-tumor activities of MAPKs inhibitors in this setting. To this purpose, here we employed P38-specific inhibitor SB202190 and JUN-specific inhibitor SP600125. The optimal concentrations of both inhibitors for each olaparib-resistant cell line were first experimentally determined (Fig. **S2**). Although individual treatment with either SB202190 or SP600125 suppressed cell growth to a comparable extent in both A2780-R and SKOV3-R cells (Fig. **S3**), the combination of both inhibitors significantly inhibited cell proliferation in a synergistic manner (Fig. **2A**, **B**). We further determined the potential influence of SB202190 and SP600125 on the cell invasive behavior by transwell assay. In addition to the suppressed cell proliferation, our results demonstrated that combinational treatment with SB202190 and SP600125 remarkably compromised the invasion capacity of olaparib-resistant cells as well (Fig. **2C**, **D**). Our data clearly indicated that MAPKs inhibitor inhibited the malignant behaviors in both cell proliferation and metastasis.

3.3. P38 and JNK Inhibition Promote Autophagy in Olaparib-resistant Ovarian Cancer Cells

To better understand the proliferation-suppressive action of MAPK inhibitors in olaparib-resistant cells, we next determined the autophagy flux in response to SB202190 and SP600125 treatment in olaparib-resistant cells. Autophagy processing was monitored by transfection of GFP-fused LC3 into olaparib-resistant ovarian cancer cells. Our western blotting results unambiguously demonstrated that combinational treatment with SB202190 and SP600125 significantly stimulated autophagy flux as indicated by the presence of LC3-phosphatidylethanolamine conjugate (LC3-II) in both A2780-R (Fig. **3A**) and SKOV3-R (Fig. **3B**). The autophagy processing was further intuitively observed by labeling the autophagic puncta structure in response to the combinational inhibitors treatment (Fig. **3C**, **D**). Our results suggested that combinational treatment with P38 and JUN inhibitors induced massive autophagy flux and eventually contributed to the suppression of cell proliferation in olaparib-resistant cells.

3.4. P38 and JNK Inhibition Decrease Epithelial-mesenchymal Transition (EMT) in Olaparib-resistant Ovarian Cancer Cells

We previously observed that combination treatment with P38 and JUN inhibitors significantly compromised the invasion capacity of olaparib-resistant ovarian cancer cells. Next, we sought to clarify its relevance to the impact on EMT process and profile the EMT markers in this setting. As shown in Fig. (**4A**), the P38 and JNK pathway inhibition remarkably decreased mesenchymal markers including N-CADHERIN and α-SMA in A2780-R, which clearly indicated the suppression of EMT processing by SB202190 and SP600125. This phenomenon was consolidated in SKOV3-R cell as well (Fig. **4B**). Further profiling of E-cadherin and

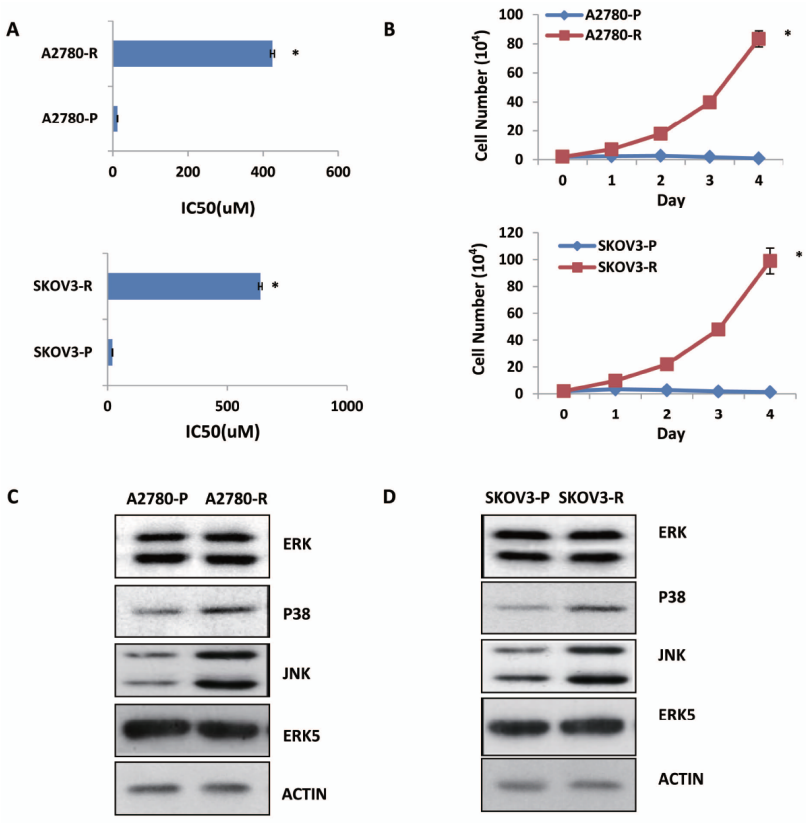

Fig. (1). P38 and JNK are overexpressed in olaparib-resistant ovarian cancer cells. (**A**) IC50 showed half maximal inhibitory concentration of olaparib in A2780-P (A2780 parental) cells, A2780-R (A2780 resistant) cells, SKOV3-P (SKOV3 parental) cells and SKOV3-R (SKOV3 resistant) cells. (**B**) Cell proliferation curve of A2780-P cells, A2780-R cells, SKOV3-P cells and SKOV3-R cells was made with the treatment of olaparib. (**C**) The proteins of MAPK family were detected in A2780-P and A2780-R cells by western blotting. (**D**) The proteins of MAPK family were detected in SKOV3-P and SKOV3-R cells by western blotting. Data information: Data are presented as mean (± SD). * P < 0.05 as compared to A2780-P or SKOV3 -P group in (A and B). The p value was calculated by Student's t-test. n = 3. Actin serves as loading control in western blotting analyses.

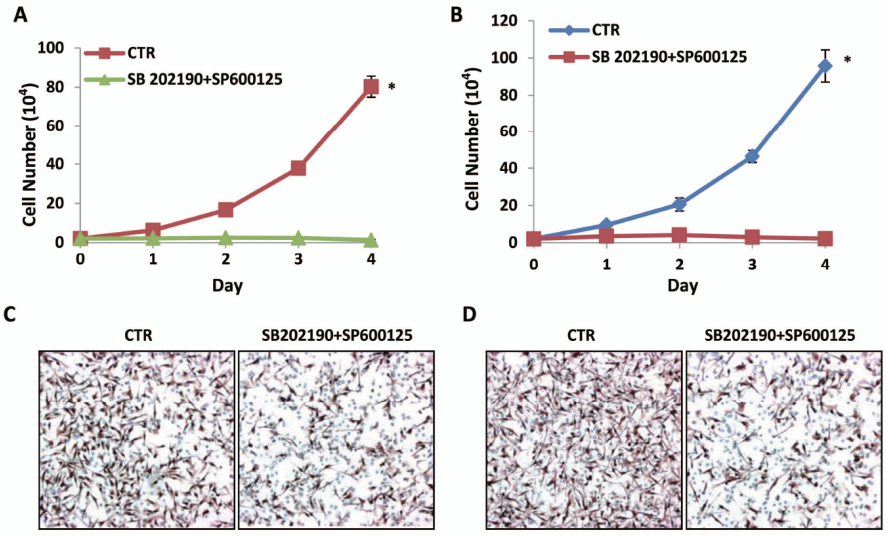

Fig. (2). P38 and JNK inhibition significantly decreases the proliferation and metastasis of olaparib-resistant ovarian cancer cells. (**A**) Cell proliferation curve of A2780-R cells was made with or without the treatment of SB202190 (p38 inhibitor, 10 μM) and SP600125 (JUN inhibitor, 10 μM). (**B**) Cell proliferation curve of SKOV3-R cells was made with or without the treatment of SB202190 and SP600125. (**C**) Stained transferred A2780-R treated with or without SB202190 and SP600125 in transwell experiment. (**D**) Stained transferred SKOV3-R cells treated with or without SB202190 and SP600125 in transwell experiment. Data information: Data are presented as mean (± SD). * P < 0.05 as compared to control group in (A and B) respectively. The p value was calculated by Student's t-test. n = 3.

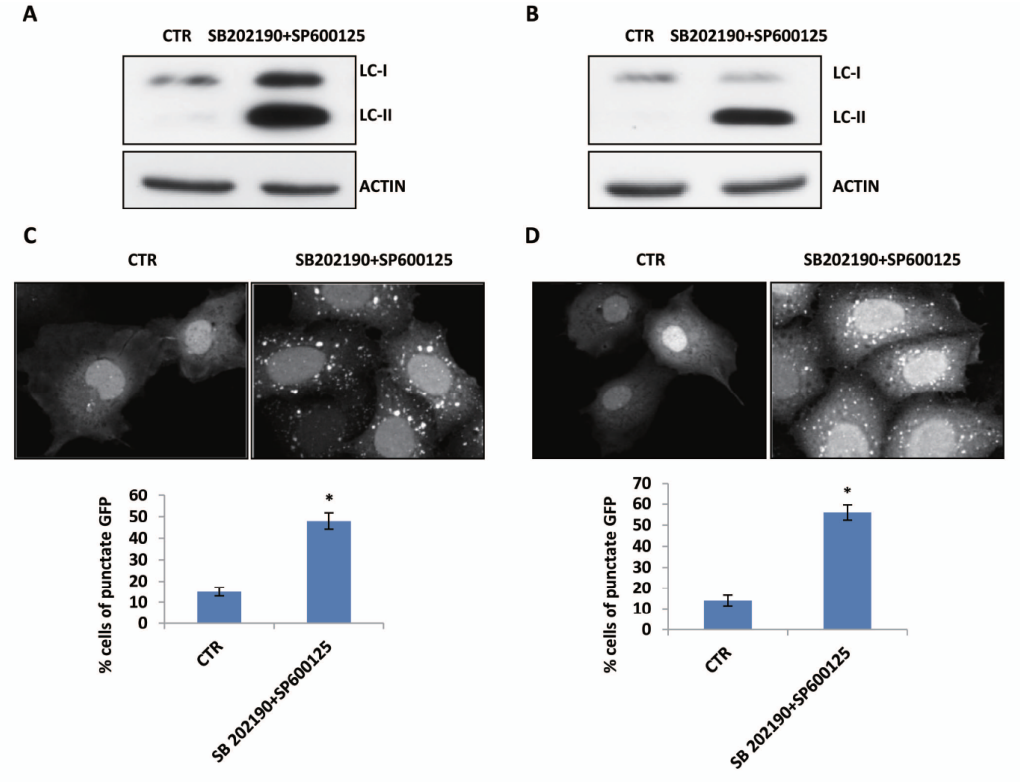

Fig. (3). P38 and JNK inhibition promotes autophagy in olaparib-resistant ovarian cancer cells. (**A**) The proteins of LC3 were detected in A2780-R treated with or without SB202190 and SP600125 by western blotting. (**B**) The proteins of LC3 were detected in SKOV3-R treated with or without SB202190 and SP600125 by western blotting. (**C**) GFP- LC3 was exogenously expressed in A2780-R. Percentage of cells exhibiting punctate fluorescence under fluorescence microscopy was calculated relative to all GFP-positive cells. (**D**) GFP- LC3 was exogenously expressed in SKOV3-R. Percentage of cells exhibiting punctate fluorescence under fluorescence microscopy was calculated relative to all GFP-positive cells. Data information: Data are presented as mean (± SD). * $P < 0.05$ as compared to control group in (C and D), respectively. The p value was calculated by Student's t-test. n = 3. Actin serves as loading control in western blotting analyses.

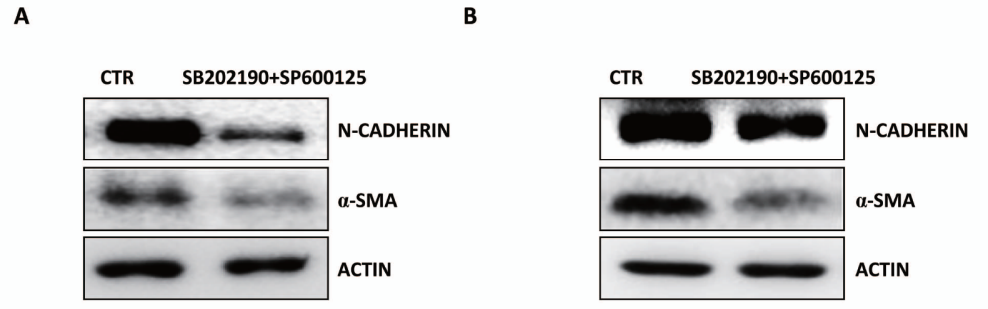

Fig. (4). P38 and JNK inhibition decrease EMT (Epithelial-Mesenchymal Transition) in olaparib-resistant ovarian cancer cells. (A) The proteins of EMT marker were detected in A2780-R treated with or without SB202190and SP600125 by western blotting. (B) The proteins of EMT marker were detected in SKOV3-R treated with or without SB202190 and SP600125 by western blotting. Actin serves as loading control in western blotting analyses.

vimentin in both cell lines in response to the combinational treatment was supplemented in Fig. (**S4**). Our results suggested that combinational treatment with SB202190 and SP600125 inhibited cell invasion through modulation of EMT processing in the olaparib-resistant ovarian cancer cells. Noteworthily, we did not observe significant changes with respect to both autophagy and EMT marker in the olaparib-resistant cells in comparison with the parental ones (Fig. **S5**).

3.5. P38 and JNK Inhibition Effectively Suppresses the Proliferation of Olaparib-resistant Ovarian Tumors *in vivo*

To exclude the potential artifacts associated with cell culture *in vitro*, we further evaluated the anti-tumor activities of P38 and JNK inhibitors *in vivo* in xenograft nude mice. Consistent with our *in vitro* observations, the xenograft tumor growth was significantly suppressed in response to combinational treatment with SB202190 and SP600125 in

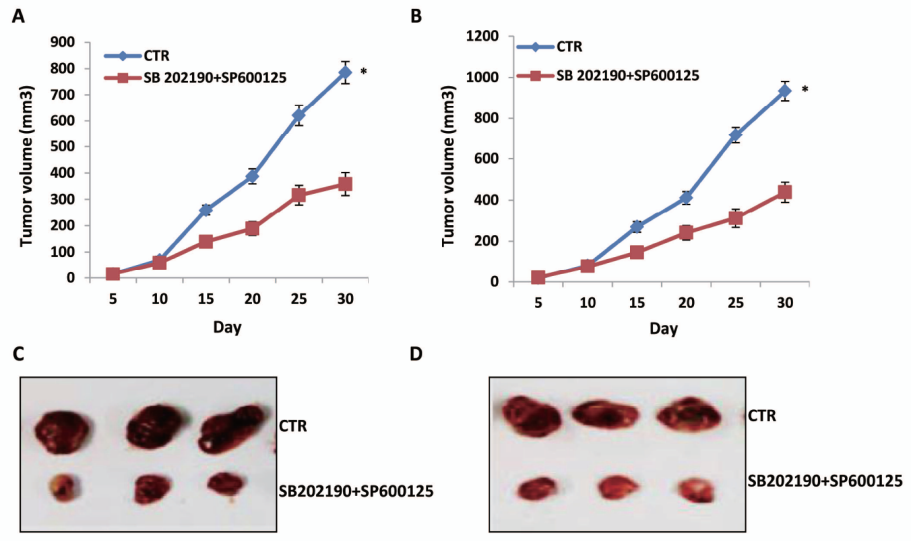

Fig. (5). P38 and JNK inhibition effectively suppresses the proliferation of olaparib-resistant ovarian tumors *in vivo*. (A.B) Tumor proliferation curves of A2780-R cells (**A**) and SKOV3-R cells (**B**) with or without the treatment of SB202190 and SP600125 *in vivo*. (C.D) Image of the final tumor of A2780-R cells (**C**) and SKOV3-R cells (**D**) with or without the treatment of SB202190 and SP600125 *in vivo*.

both A2780-R- and SKOV3-R-recipient mice (Fig. **5A** and **B**). The representative macroscopic images of xenograft tumor at the endpoint of the experiment are shown in Fig. (**5C**) and D. Therefore, we observed consistent outcome *in vivo* by the employment of xenograft mice. Taken together, our data uncovered the significant anti-tumor effect of P38 and JNK inhibitors in olaparib-resistant ovarian cancer.

4. DISCUSSION

Olaparib was approved for use as a single agent for advanced ovarian cancer that previously received three or more prior lines of chemotherapy and with germline BRCA mutations by the FDA in 2014 [12]. Although clinical benefits have been observed in some patients, most cases manifested intrinsic drug resistance. Moreover, initial responders later developed resistance as well during disease progression. Therefore, to better understand the molecular mechanism underlying drug resistance and seeking for the potential compounds to surmount olaparib resistance is in urgent need with respect to the clinical application of this target therapeutics. To this purpose, here we first generated the olaparib-resistant human ovarian cancer cell lines in both A2780 and SKOV3. The success in the establishment of resistant cells was validated by cytotoxic MTT assay. Cell proliferation was significantly higher in resistant cell lines in comparison with sensitive counterparts upon challenged with olaparib. Notably, here we characterized that MAPK pathway was aberrantly up-regulated in olaparib-resistant cells, which might link to the drug resistance in this disease. We next dosed olaparib-resistant cells with MAPK inhibitors including P38-specific SB202190 and JUN-specific SP600125. Our results demonstrated that combinational treatment with these two inhibitors significantly inhibited cell proliferation and invasive capacity. Furthermore, we provided experimental evidence supporting that the combination of SB202190 and SP600125 stimulated autophagy flux in olaparib-resistant cells, which predominantly underlaid its suppressive effects on cell proliferation. We also clarified that the compromised cell invasion capacity was intimately associated with the modulation on EMT process. Most importantly, all of our *in vitro* observations were consolidated *in vivo* using the xenograft tumor mice, wherein administration of both P38 inhibitor and JUN inhibitor greatly retarded tumor progression in the olaparib-resistant human ovarian cancer cell recipient animals. Therefore, we well-recapitulated olaparib resistance *in vitro* and identified aberrant overexpression of P38 and JUN associated with this phenomenon, and most significantly, our data highlighted the potential therapeutic value of MAPK inhibitors in the treatment of olaparib-resistant ovarian cancer, which might hold great clinical promise and further investigations are warranted.

Aberrant activation of MAPK pathway is frequently linked to drug resistance in a variety of human malignancies. For instance, Chocry *et al.* demonstrated that inhibition of P38 MAPK in colorectal cancer cell lines reversed its resistance to oxaliplatin [13]. Jain *et al.* showed that combinational targeting of MAPK and PI3K/mTOR signaling pathways overcame resistance to single-agent therapy for oncogenic BRAF gene fusions [14]. In non-small cell lung cancer, Wang *et al.* suggested that lncRNA SNHG12 contributed to multidrug resistance through the activation of the MAPK/Slug pathway by sponging miR-181a [15]. Yin *et al.* showed that GPER promoted tamoxifen-resistance in ER+ breast cancer cells by reduced Bim proteins through MAPK/Erk-TRIM2 signaling axis [16]. In addition, the activated MAPK/Erk/Bim signaling pathway was demonstrated to be associated with Reg4 enhanced 5-fluorouracil resistance in gastric cancer [17]. Resistance to tyrosine kinase inhibitors was also conferred by aberrant activation of the MAPK pathway *via* stimulating EGFR transcription and EGFR dephosphorylation [16]. In colorectal cancer, Ma *et al.* demonstrated that MAPK pathway regulated intrinsic resistance to BET inhibitors [18]. Likewise, here we demonstrated that

P38 and JNK pathways were significantly activated in olaparib resistant ovarian cancer cells, which might consequently contribute to intrinsic drug resistance. However, the molecular mechanism underlying over-activation of MAPK signaling in olaparib-resistant cancer cells is still elusive. Vaidyanathan *et al.* reported that ABCB1 was significantly induced in olaparib-resistant cancer cells [19], which was subsequently demonstrated to stimulate downstream phosphorylation cascade including Akt, ERK1/2, p38 MAPK and JNK [20]. Therefore, we hypothesize that ABCB1 may play a critical role in the aberrant activation of the MAPK pathway in olaparib-resistant cancers, which definitely warrants further investigations.

The anti-tumor activities of P38-specific inhibitor SB202190 and JUN-specific inhibitor SP600125 have been extensively investigated nowadays. For example, Nemoto *et al.* first reported that SB202190 induced cell apoptosis through inhibition of P38beta mitogen-activated protein kinase [21]. Hamanoue *et al.* demonstrated a combination of SB202190 and SB203580 induced apoptosis in cultured mature oligodendrocytes *via* P38 pathway inhibition [22]. In breast cancer MDA-MB-231 cell line, Duzqun *et al.* showed that SB202190 was more effective than SB203580 with respect to the inhibition of cell proliferation and cell migration [23]. Karahashi *et al.* reported the apoptotic cell death-inducing effect of SB202190 in lipopolysaccharide-treated macrophage-like cells [24]. Likewise, Mili *et al.* suggested the effect of SP600125 on the mitotic spindle in HeLa cells, which led to the mitotic arrest, endoreduplication and cell apoptosis [25]. Application of SP600125 overcame antimitotic drug-resistance in cancer cells by increasing apoptosis with the independence of P-gp inhibition [26]. Lin *et al.* demonstrated that SP600125 enhanced TGF-β-induced apoptosis of RBE human cholangiocarcinoma cells in a Smad-dependent manner [27]. Jemaa *et al.* showed the selective killing action of SP600125 against p53-deficient cancer cells [28]. In view of the overexpression of both P38 and JNK in olaparib-resistant ovarian cancer cells, here we combined SB202190 and SP600125 together for the therapeutic purpose, which manifested significant inhibition of cell proliferation and invasion *in vitro* and suppression of xenograft tumor growth *in vivo*. Our data highlighted the potential therapeutic value of combinational SB202190 and SP600125 against olaparib-resistant ovarian cancer, which might hold great promise for this disease.

LIST OF ABBREVIATIONS

ANOVA	=	One-way Analysis of Variance
ATCC	=	The American Type Culture Collection
CCK-8	=	Cell Counting Kit-8
EMT	=	Epithelial-Mesenchymal Transition
MAPK	=	Mitogen-Activated Protein Kinase
PARP	=	Poly ADP ribose polymerase

ETHICS APPROVAL AND CONSENT TO PARTICIPATE

Not applicable.

HUMAN AND ANIMAL RIGHTS

No Animals/Humans were used for studies that are the basis of this research.

CONSENT FOR PUBLICATION

Not applicable.

CONFLICT OF INTEREST

The authors declare no conflict of interest, financial or otherwise.

ACKNOWLEDGMENTS

This study was supported by the Key Research and Development Program of Shandong Province (2015GSF118140).

SUPPLEMENTARY MATERIAL

Supplementary material is available on the publisher's website along with the published article.

REFERENCES

[1] Jayson, G.C.; Kohn, E.C.; Kitchener, H.C.; Ledermann, J.A. Ovarian cancer. *Lancet,* **2014**, *384* (9951), 1376-1388.

[2] Siegel, R. L.; Miller, K. D.; Jemal, A. Cancer Statistics, 2017. *CA Cancer J Clin,* **2017**, *67* (1), 7-30.

[3] Hunn, J.; Rodriguez, G. C. Ovarian cancer: etiology, risk factors, and epidemiology. *Clin Obstet Gynecol,* **2012**, *55* (1), 3-23.

[4] 4. Rebbeck, T. R.; Mitra, N.; Wan, F.; Sinilnikova, O. M.; Healey, S.; McGuffog, L.; Mazoyer, S.; Chenevix-Trench, G.; Easton, D. F.; Antoniou, A. C.; Nathanson, K. L.; Consortium, C.; Laitman, Y.; Kushnir, A.; Paluch-Shimon, S.; Berger, R.; Zidan, J.; Friedman, E.; Ehrencrona, H.; Stenmark-Askmalm, M.; Einbeigi, Z.; Loman, N.; Harbst, K.; Rantala, J.; Melin, B.; Huo, D.; Olopade, O. I.; Seldon, J.; Ganz, P. A.; Nussbaum, R. L.; Chan, S. B.; Odunsi, K.; Gayther, S. A.; Domchek, S. M.; Arun, B. K.; Lu, K. H.; Mitchell, G.; Karlan, B. Y.; Walsh, C.; Lester, J.; Godwin, A. K.; Pathak, H.; Ross, E.; Daly, M. B.; Whittemore, A. S.; John, E. M.; Miron, A.; Terry, M. B.; Chung, W. K.; Goldgar, D. E.; Buys, S. S.; Janavicius, R.; Tihomirova, L.; Tung, N.; Dorfling, C. M.; van Rensburg, E. J.; Steele, L.; Neuhausen, S. L.; Ding, Y. C.; Ejlertsen, B.; Gerdes, A. M.; Hansen, T.; Ramon y Cajal, T.; Osorio, A.; Benitez, J.; Godino, J.; Tejada, M. I.; Duran, M.; Weitzel, J. N.; Bobolis, K. A.; Sand, S. R.; Fontaine, A.; Savarese, A.; Pasini, B.; Peissel, B.; Bonanni, B.; Zaffaroni, D.; Vignolo-Lutati, F.; Scuvera, G.; Giannini, G.; Bernard, L.; Genuardi, M.; Radice, P.; Dolcetti, R.; Manoukian, S.; Pensotti, V.; Gismondi, V.; Yannoukakos, D.; Fostira, F.; Garber, J.; Torres, D.; Rashid, M. U.; Hamann, U.; Peock, S.; Frost, D.; Platte, R.; Evans, D. G.; Eeles, R.; Davidson, R.; Eccles, D.; Cole, T.; Cook, J.; Brewer, C.; Hodgson, S.; Morrison, P. J.; Walker, L.; Porteous, M. E.; Kennedy, M. J.; Izatt, L.; Adlard, J.; Donaldson, A.; Ellis, S.; Sharma, P.; Schmutzler, R. K.; Wappenschmidt, B.; Becker, A.; Rhiem, K.; Hahnen, E.; Engel, C.; Meindl, A.; Engert, S.; Ditsch, N.; Arnold, N.; Plendl, H. J.; Mundhenke, C.; Niederacher, D.; Fleisch, M.; Sutter, C.; Bartram, C. R.; Dikow, N.; Wang-Gohrke, S.; Gadzicki, D.; Steinemann, D.; Kast, K.; Beer, M.; Varon-Mateeva, R.; Gehrig, A.; Weber, B. H.; Stoppa-Lyonnet, D.; Sinilnikova, O. M.; Mazoyer, S.; Houdayer, C.; Belotti, M.; Gauthier-Villars, M.; Damiola, F.; Boutry-Kryza, N.; Lasset, C.; Sobol, H.; Peyrat, J. P.; Muller, D.; Fricker, J. P.; Collonge-Rame, M. A.; Mortemousque, I.; Nogues, C.; Rouleau, E.; Isaacs, C.; De Paepe, A.; Poppe, B.; Claes, K.; De Leeneer, K.; Piedmonte, M.; Rodriguez, G.; Wakely, K.; Boggess, J.; Blank, S. V.; Basil, J.; Azodi, M.; Phillips, K. A.; Caldes, T.; de la Hoya, M.; Romero, A.; Nevanlinna, H.; Aittomaki, K.; van der Hout, A. H.; Hogervorst, F. B.; Verhoef, S.; Collee, J. M.; Seynaeve, C.; Oosterwijk, J. C.; Gille, J. J.; Wijnen, J. T.; Gomez Garcia, E. B.; Kets, C. M.; Ausems, M. G.; Aalfs, C. M.; Devilee, P.; Mensenk-

amp, A. R.; Kwong, A.; Olah, E.; Papp, J.; Diez, O.; Lazaro, C.; Darder, E.; Blanco, I.; Salinas, M.; Jakubowska, A.; Lubinski, J.; Gronwald, J.; Jaworska-Bieniek, K.; Durda, K.; Sukiennicki, G.; Huzarski, T.; Byrski, T.; Cybulski, C.; Toloczko-Grabarek, A.; Zlowocka-Perlowska, E.; Menkiszak, J.; Arason, A.; Barkardottir, R. B.; Simard, J.; Laframboise, R.; Montagna, M.; Agata, S.; Alducci, E.; Peixoto, A.; Teixeira, M. R.; Spurdle, A. B.; Lee, M. H.; Park, S. K.; Kim, S. W.; Friebel, T. M.; Couch, F. J.; Lindor, N. M.; Pankratz, V. S.; Guidugli, L.; Wang, X.; Tischkowitz, M.; Foretova, L.; Vijai, J.; Offit, K.; Robson, M.; Rau-Murthy, R.; Kauff, N.; Fink-Retter, A.; Singer, C. F.; Rappaport, C.; Gschwantler-Kaulich, D.; Pfeiler, G.; Tea, M. K.; Berger, A.; Greene, M. H.; Mai, P. L.; Imyanitov, E. N.; Toland, A. E.; Senter, L.; Bojesen, A.; Pedersen, I. S.; Skytte, A. B.; Sunde, L.; Thomassen, M.; Moeller, S. T.; Kruse, T. A.; Jensen, U. B.; Caligo, M. A.; Aretini, P.; Teo, S. H.; Selkirk, C. G.; Hulick, P. J.; Andrulis, I. Association of type and location of BRCA1 and BRCA2 mutations with risk of breast and ovarian cancer. *JAMA,* **2015**, *313*(13), 1347-1361.

[5] Sung, H. K.; Ma, S. H.; Choi, J. Y.; Hwang, Y.; Ahn, C.; Kim, B. G.; Kim, Y. M.; Kim, J. W.; Kang, S.; Kim, J.; Kim, T. J.; Yoo, K. Y.; Kang, D.; Park, S. The Effect of Breastfeeding Duration and Parity on the Risk of Epithelial Ovarian Cancer: A Systematic Review and Meta-analysis. *J Prev Med Public Health,* **2016**, *49*(6), 349-366.

[6] Bookman, M. A. Optimal primary therapy of ovarian cancer. *Ann Oncol,* **2016**, *27 Suppl 1*, i58-i62.

[7] Bookman, M. A. First-line chemotherapy in epithelial ovarian cancer. *Clin Obstet Gynecol,* **2012**, *55* (1), 96-113.

[8] Zsiros, E.; Tanyi, J.; Balint, K.; Kandalaft, L. E. Immunotherapy for ovarian cancer: recent advances and perspectives. *Curr Opin Oncol,* **2014**, *26* (5), 492-500.

[9] Pujade-Lauraine, E.; Combe, P. [Olaparib in ovarian cancer with BRCA mutation]. *Bull Cancer,* **2015**, *102* (6 Suppl 1), S82-84.

[10] Gunderson, C. C.; Moore, K. N. Olaparib: an oral PARP-1 and PARP-2 inhibitor with promising activity in ovarian cancer. *Future Oncol,* **2015**, *11* (5), 747-757.

[11] Chen, Y.; Zhang, L.; Hao, Q. Olaparib: a promising PARP inhibitor in ovarian cancer therapy. *Arch Gynecol Obstet,* **2013**, *288* (2), 367-374.

[12] Deeks, E. D. Olaparib: first global approval. *Drugs,* **2015**, *75* (2), 231-240.

[13] Chocry, M.; Leloup, L.; Kovacic, H. Reversion of resistance to oxaliplatin by inhibition of p38 MAPK in colorectal cancer cell lines: involvement of the calpain / Nox1 pathway. *Oncotarget,* **2017**, *8* (61), 103710-103730.

[14] Jain, P.; Silva, A.; Han, H. J.; Lang, S. S.; Zhu, Y.; Boucher, K.; Smith, T. E.; Vakil, A.; Diviney, P.; Choudhari, N.; Raman, P.; Busch, C. M.; Delaney, T.; Yang, X.; Olow, A. K.; Mueller, S.; Haas-Kogan, D.; Fox, E.; Storm, P. B.; Resnick, A. C.; Waanders, A. J. Overcoming resistance to single-agent therapy for oncogenic BRAF gene fusions *via* combinatorial targeting of MAPK and PI3K/mTOR signaling pathways. *Oncotarget,* **2017**, *8* (49), 84697-84713.

[15] Wang, P.; Chen, D.; Ma, H.; Li, Y. LncRNA SNHG12 contributes to multidrug resistance through activating the MAPK/Slug pathway by sponging miR-181a in non-small cell lung cancer. *Oncotarget,* **2017**, *8* (48), 84086-84101.

[16] Yin, N.; Lepp, A.; Ji, Y.; Mortensen, M.; Hou, S.; Qi, X. M.; Myers, C. R.; Chen, G. The K-Ras effector p38gamma MAPK confers intrinsic resistance to tyrosine kinase inhibitors by stimulating EGFR transcription and EGFR dephosphorylation. *J Biol Chem,* **2017**, *292* (36), 15070-15079.

[17] Jin, J.; Lv, H.; Wu, J.; Li, D.; Chen, K.; Zhang, F.; Han, J.; Feng, J.; Zhang, N.; Yu, H.; Su, D.; Ying, L. Regenerating Family Member 4 (Reg4) Enhances 5-Fluorouracil Resistance of Gastric Cancer Through Activating MAPK/Erk/Bim Signaling Pathway. *Med Sci Monit,* **2017**, *23*, 3715-3721.

[18] Ma, Y.; Wang, L.; Neitzel, L. R.; Loganathan, S. N.; Tang, N.; Qin, L.; Crispi, E. E.; Guo, Y.; Knapp, S.; Beauchamp, R. D.; Lee, E.; Wang, J. The MAPK Pathway Regulates Intrinsic Resistance to BET Inhibitors in Colorectal Cancer. *Clin Cancer Res,* **2017**, *23* (8), 2027-2037.

[19] Vaidyanathan, A.; Sawers, L.; Gannon, A. L.; Chakravarty, P.; Scott, A. L.; Bray, S. E.; Ferguson, M. J.; Smith, G. ABCB1 (MDR1) induction defines a common resistance mechanism in paclitaxel- and olaparib-resistant ovarian cancer cells. *Br J Cancer,* **2016**, *115* (4), 431-441.

[20] Satonaka, H.; Ishida, K.; Takai, M.; Koide, R.; Shigemasa, R.; Ueyama, J.; Ishikawa, T.; Hayashi, K.; Goto, H.; Wakusawa, S. (-)-Epigallocatechin-3-gallate Down-regulates Doxorubicin-induced Overexpression of P-glycoprotein Through the Coordinate Inhibition of PI3K/Akt and MEK/ERK Signaling Pathways. *Anticancer Res,* **2017**, *37* (11), 6071-6077.

[21] Nemoto, S.; Xiang, J.; Huang, S.; Lin, A. Induction of apoptosis by SB202190 through inhibition of p38beta mitogen-activated protein kinase. *J Biol Chem,* **1998**, *273* (26), 16415-16420.

[22] Hamanoue, M.; Sato, K.; Takamatsu, K. Inhibition of p38 mitogen-activated protein kinase-induced apoptosis in cultured mature oligodendrocytes using SB202190 and SB203580. *Neurochem Int,* **2007**, *51* (1), 16-24.

[23] Duzgun, S. A.; Yerlikaya, A.; Zeren, S.; Bayhan, Z.; Okur, E.; Boyaci, I. Differential effects of p38 MAP kinase inhibitors SB203580 and SB202190 on growth and migration of human MDA-MB-231 cancer cell line. *Cytotechnology,* **2017**, *69* (4), 711-724.

[24] Karahashi, H.; Nagata, K.; Ishii, K.; Amano, F. A selective inhibitor of p38 MAP kinase, SB202190, induced apoptotic cell death of a lipopolysaccharide-treated macrophage-like cell line, J774.1. *Biochim Biophys Acta,* **2000**, *1502* (2), 207-223.

[25] Mili, D.; Abid, K.; Rjiba, I.; Kenani, A. Effect of SP600125 on the mitotic spindle in HeLa Cells, leading to mitotic arrest, endoreduplication and apoptosis. *Mol Cytogenet,* **2016**, *9*, 86.

[26] Kim, J. H.; Chae, M.; Choi, A. R.; Sik Kim, H.; Yoon, S. SP600125 overcomes antimitotic drug-resistance in cancer cells by increasing apoptosis with independence of P-gp inhibition. *Eur J Pharmacol,* **2014**, *723*, 141-147.

[27] Lin, Y.; Zhang, B.; Liang, H.; Lu, Y.; Ai, X.; Zhang, B.; Chen, X. JNK inhibitor SP600125 enhances TGF-beta-induced apoptosis of RBE human cholangiocarcinoma cells in a Smad-dependent manner. *Mol Med Rep,* **2013**, *8* (6), 1623-1629.

[28] Jemaa, M.; Vitale, I.; Kepp, O.; Berardinelli, F.; Galluzzi, L.; Senovilla, L.; Marino, G.; Malik, S. A.; Rello-Varona, S.; Lissa, D.; Antoccia, A.; Tailler, M.; Schlemmer, F.; Harper, F.; Pierron, G.; Castedo, M.; Kroemer, G. Selective killing of p53-deficient cancer cells by SP600125. *EMBO Mol Med,* **2012**, *4* (6), 500-514.

PMID: 30003858